

ARTICLE

Supplementary Information

Received 00th January 20xx,  
 Accepted 00th January 20xx

DOI: 10.1039/x0xx00000x

High Yield Exfoliation of a Sub-Micron hexagonal Boron Nitride  
 Using a Solvent Free Method

Diana Santiago,<sup>b</sup> Maricela Lizcano,<sup>b</sup> Sean P. McDarby,<sup>a</sup>  
 Ching-Cheh Hung,<sup>c</sup> and Baochau N. Nguyen<sup>\*a</sup>

**Table S1** (002) peak position and (002) FWHM of  $A_I$ -Cl and  $A_I$ -F

	(002) Peak position	(002) FWHM
<b>A</b> – pristine <i>h</i> BN	26.707	0.378
<b>A<sub>I</sub></b> -LiCl	26.571	0.483
<b>A<sub>I</sub></b> -NaCl	26.667	0.461
<b>A<sub>I</sub></b> -KCl	26.686	0.487
<b>A<sub>I</sub></b> -LiF	26.457	0.469
<b>A<sub>I-H</sub></b> -NaF	26.628	0.485
<b>A<sub>I-H</sub></b> -KF	26.571	0.487

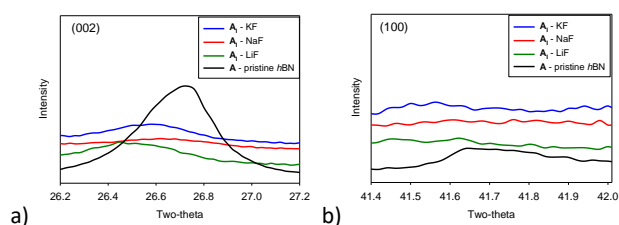


**Figure S1** (a) and (b) XRD patterns of intercalated  $A_I$ -F on both (002) and (100) planes, respectively, using fluoride salts as activation agents. Note that (002) plane of pristine *h*BN was scaled down for observation and comparison to the exfoliated  $A_I$ -Cl.

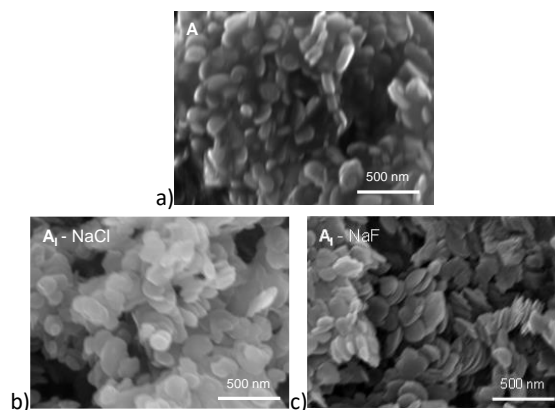


**Figure S2** SEM images of (a) pristine *h*BN, (b) intercalated  $A_I$  using NaCl and (c) intercalated  $A_I$  using NaF as activation agents.

<sup>a</sup> Universities Space Research Association, 425 3<sup>rd</sup> Street SW, Suite 950, Washington DC 20024. E-mail: [Baochau.n.nguyen@nasa.gov](mailto:Baochau.n.nguyen@nasa.gov); Tel: +1-216-433-2738

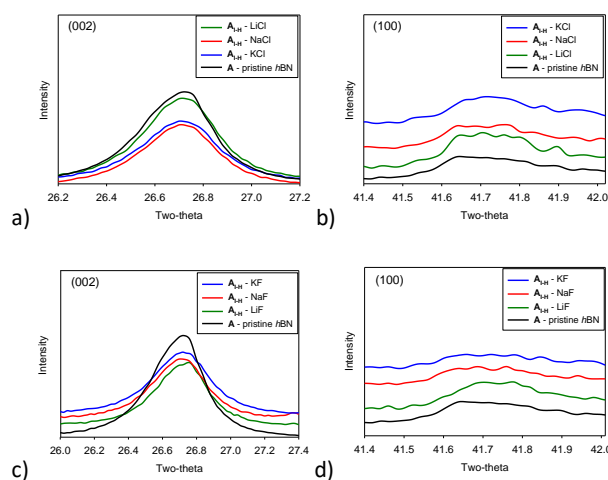
<sup>b</sup> NASA Glenn Research Center, 21000 Brookpark Road, Cleveland, OH, 44135. E-mail: [diana.santiago-dejesus@nasa.gov](mailto:diana.santiago-dejesus@nasa.gov); Tel: +1-216-433-6068.

<sup>c</sup> Boron Nitride Research and Engineering, LCC, Orlando, FL, 32827.

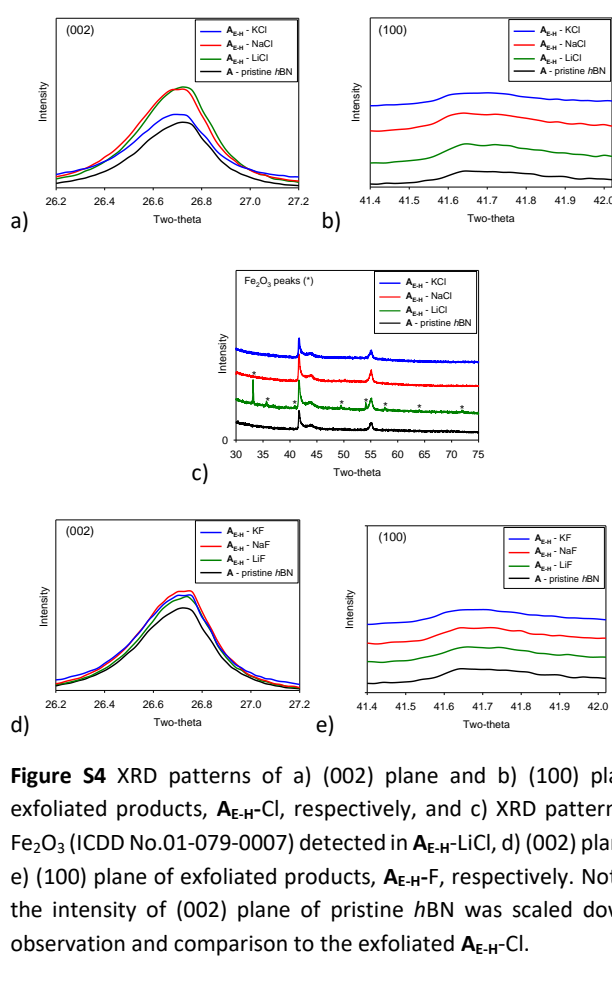
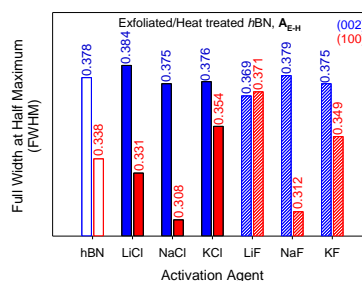
\*Corresponding author

**Table S2** (002) peak position and (002) FWHM of  $A_{I-H-Cl}$  and  $A_{I-H-F}$ 

	(002) Peak position	(002) FWHM
A – pristine <i>h</i> BN	26.707	0.378
$A_{I-H-LiCl}$	26.707	0.389
$A_{I-H-NaCl}$	26.707	0.335
$A_{I-H-KCl}$	26.707	0.357
$A_{I-H-LiF}$	26.745	0.362
$A_{I-H-NaF}$	26.726	0.389
$A_{I-H-KF}$	26.707	0.386

**Figure S3** XRD patterns of a) (002) plane and b) (100) plane of exfoliated products,  $A_{I-H-Cl}$ , c) (002) plane and d) (100) plane of exfoliated products,  $A_{I-H-F}$ , respectively. Note that the intensity of (002) plane of pristine *h*BN was scaled down for observation and comparison to the exfoliated  $A_{E-H-Cl}$ .**Table S3** (002) peak position of  $A_{E-H-Cl}$  and  $A_{E-H-F}$ 

	(002) Peak position
A – pristine <i>h</i> BN	26.707
$A_E-LiCl$	26.724
$A_E-NaCl$	26.707
$A_E-KCl$	26.688
$A_E-LiF$	26.745
$A_E-NaF$	26.707
$A_E-KF$	26.707

**Figure S4** XRD patterns of a) (002) plane and b) (100) plane of exfoliated products,  $A_{E-H-Cl}$ , respectively, and c) XRD pattern of  $\alpha$ - $Fe_2O_3$  (ICDD No.01-079-0007) detected in  $A_{E-H-LiCl}$ , d) (002) plane and e) (100) plane of exfoliated products,  $A_{E-H-F}$ , respectively. Note that the intensity of (002) plane of pristine *h*BN was scaled down for observation and comparison to the exfoliated  $A_{E-H-Cl}$ .**Figure S5** Full Width at Half Maximum (FWHM) of (002) and (100) planes of exfoliated/heat treated,  $A_{E-H}$ .**Table S4** % yield of  $A_{E-H}$  with different activation agents

$A_{E-H}$	% Yield
$A_{E-H-LiCl}$	>100
$A_{E-H-NaCl}$	>100
$A_{E-H-KCl}$	>100
$A_{E-H-LiF}$	93.0
$A_{E-H-NaF}$	83.6
$A_{E-H-KF}$	91.0

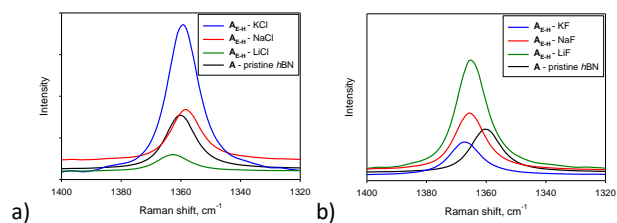


**Figure S6** Raman spectroscopy of a)  $A_{E-H-Cl}$  and b)  $A_{E-H-F}$ , compared to **A**.

**Table S5** Raman peak shift, peak height and FWHM of  $A_{E-H-Cl}$  and  $A_{E-H-F}$

	Peak shift ( $cm^{-1}$ )	Peak height	FWHM
<b>A</b> – pristine <i>h</i> BN	1360.2	2404	11.8
$A_{E-H-LiCl}$	1362.8	723	13.6
$A_{E-H-NaCl}$	1358.3	2242	11.9
$A_{E-H-KCl}$	1359.3	6541	12.1
$A_{E-H-LiF}$	1365.1	5986	13.5
$A_{E-H-NaF}$	1365.5	3071	11.0
$A_{E-H-KF}$	1367.2	1725	10.7